Diffusive single and multiply connected SNS systems with high-transparent interfaces

T I Baturina, Z D Kvon, A E Plotnikov,
R Donaton, M R Baklanov

Abstract. We present low-temperature transport measurements on single and multiply connected SNS systems fabricated on the basis of superconducting polycrystalline PtSi film. Zero bias anomaly (ZBA) and subharmonic energy gap structure (SGS) originating from the proximity effects and the multiple Andreev reflections were observed and carefully studied. It was found that the ZBA is not described by any theories developed for SNS junctions with high-transparent NS interface. The value of excess conductance and the width of ZBA for single SNS junction far exceed values predicted by up-to-date theories.

The NS interfaces of our SNS junctions are really high-transparent, for superconducting and normal metal parts are made of the same material. On the other hand, as we have to deal with long diffusive SNS junctions one might expect that impurities could provide the conditions for incoherent multiple Andreev reflections.

In comparison with single SNS junctions we observe significant narrowing of the ZBA in multiply connected SNS systems: one-dimensional (1D) and two-dimensional arrays (2D) of SNS junctions. In 2D arrays an appreciable SGS appears, with up to $n = 16$ ($eV = \pm 2\Delta/n$) and some numbers being lost. One of the most interesting results obtained on 1D arrays consists in the appearance of symmetrical dips on the dependences $\mathrm{d}V/\mathrm{d}I - V$ at dc voltage corresponding to some multiples of Δ/e. Presented results show that coherent phenomena governed by Andreev reflection are not self-averaging and are maintained over a macroscopic scale.

Rapid progress in fabrication techniques has made it possible to produce mesoscopic hybrid structures and to investigate phase-coherent transport in them. In the past few years, the mesoscopic systems, consisting of a normal metal (N) or heavily doped semiconductor being in contact with a superconductor (S), have been attracting an increasing interest mainly because of the richness of involved quantum effects [1]. The key mechanism governing the carrier transport through the NS contact is the Andreev reflection. In this process, an electron-like excitation with an energy ϵ smaller than the superconducting gap Δ moving from the normal metal to the NS interface is retro-reflected as a hole-like excitation, while Cooper pair is transmitted into the superconductor. This phenomenon is the basis of the proximity effect, which generally implies the influence of a superconductor on the properties of a normal metal being in electrical contact. Nowadays, the actual proximity effect is considered to be determined by the parameters of the normal part of the junction and by the properties of the NS interface in common. SNS systems may be classified with respect to the relation between the mean free path and any other characteristic length in the system (either diffusive or ballistic regime) and by the transparency of the NS interfaces. At present, a large variety of NS and SNS junctions (most of them are diffusive) is fabricated and studied [2 – 13]. The investigations of these junctions are primarily focused on the nonlinear behavior of current – voltage characteristics, which exhibit the zero bias anomaly, the subharmonic energy gap structure (SGS), etc. Although much work has been done on single SNS junctions, it is an experimental challenge to fabricate and carry out comparative measurements on multiply connected SNS systems. In the present paper, we report the results of low-temperature transport measurements on single and multiply connected SNS systems (two-dimensional and one-dimensional arrays of SNS junctions) and perform the comparative analysis of their properties.

The design of our samples is based on the technique of fabrication of SNS junctions with perfect NS interfaces that has been recently proposed and realized in our work [13]. The idea of our method is to use the fact that superconductivity of ultrathin polycrystalline PtSi films is destroyed inside submicron constriction made out of such film by means of electron beam lithography and subsequent plasma etching. The reason for this superconductivity suppression is not quite clear. Nevertheless, it allows us to prepare SNS junctions where both superconductive and normal parts are made from the same material, thus avoiding usual uncertainty in parameters of electron transport through an NS interface between two different materials, where uncontrollable oxide barriers or extra concentration of disorder are typical. This approach *a priori* suggests high transparency of the NS interfaces of our SNS junctions.

The original PtSi film with thickness of 6 nm was formed on Si substrate. The film had critical temperature $T_c = 0.56\,\mathrm{K}$. The resistance per square was 104 Ω. The carrier density obtained from Hall measurements was $7 \times 10^{22}\ \mathrm{cm}^{-3}$, corresponding to the mean free path $l = 1.2$ nm and the diffusion constant $D = 6\ \mathrm{cm}^2\ \mathrm{s}^{-1}$ estimated assuming the simple free-electron model. The initial samples used in the experiments were Hall bridges with 50 μm in width and 100 μm in length.

The hybrid SNS structures were designed to provide the possibility of the comparative study. Single SNS junction is the 0.4 μm constriction made in film and placed in the Hall bridge. A scanning electron micrograph and a schematic view of a sample showing the dimensions are presented in Fig. 1a,b. To fabricate 2D array we patterned the square lattice of holes covering the whole Hall bridge by means of electron lithography and subsequent plasma etching. The micrograph of the lattice is shown in Fig. 2a. The lattice constant is 2.1 μm and the diameter of holes is 1.7 μm, so the width of the smallest part is 0.4 μm. Thus we obtain the structure which consists of the islands of the film, with the characteristic dimension being 1.3 μm, connected by narrow necks. As the constrictions are not superconducting we have a 2D array of SNS junctions (Fig. 2b). In the similar way 1D arrays of SNS junctions were fabricated with the same characteristic dimensions (see Fig. 3a,b).

The differential resistance measurements are performed using a conventional four-terminal ac lock-in technique, with ac currents of 1 – 10 nA at a frequency of ~ 10 Hz. Figure 1c shows typical dependences of $\mathrm{d}V/\mathrm{d}I$ on V for the structures with a single SNS junction. The data exhibit a behavior very similar to that reported in the previous work [13]. The differential resistance reveals a minimum at zero bias voltage

T I Baturina, Z D Kvon, A E Plotnikov, M R Baklanov Institute of Semiconductor Physics, Siberian Division of RAS, 630090 Novosibirsk, Russian Federation
R Donaton, M R Baklanov IMEC, Kapeldreef 75, B-3001 Leuven, Belgium

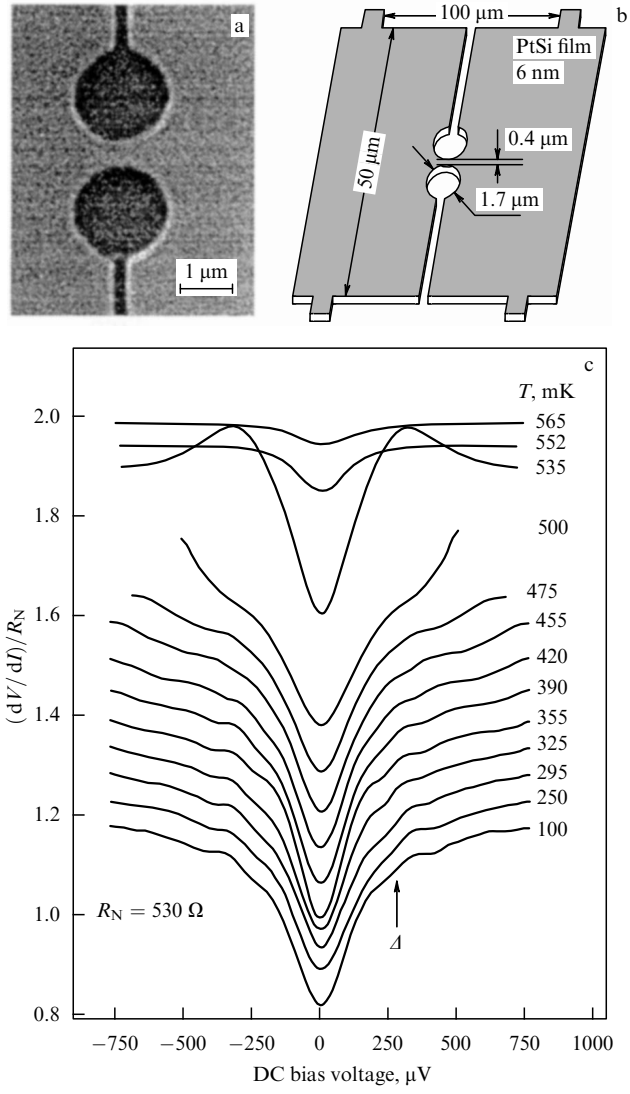

Figure 1. (a) Scanning electron micrograph of the sample with single constriction formed by electron beam lithography and subsequent plasma etching of the 6 nm PtSi film grown on Si substrate. (b) Schematic view of a junction (not to scale) showing the layout of the constriction in the Hall bridge. (c) Normalized differential resistance $(dV/dI)/R_N$ of a single SNS junction as a function of bias voltage at different temperatures. (All traces except the lowest trace are successively shifted upward by 0.05, for clarity.) The subharmonic energy gap structure is smeared and can be seen more clearly in the dependence of d^2V/dI^2 on V. The arrow indicates $eV = \Delta$ corresponding to the maximum slope.

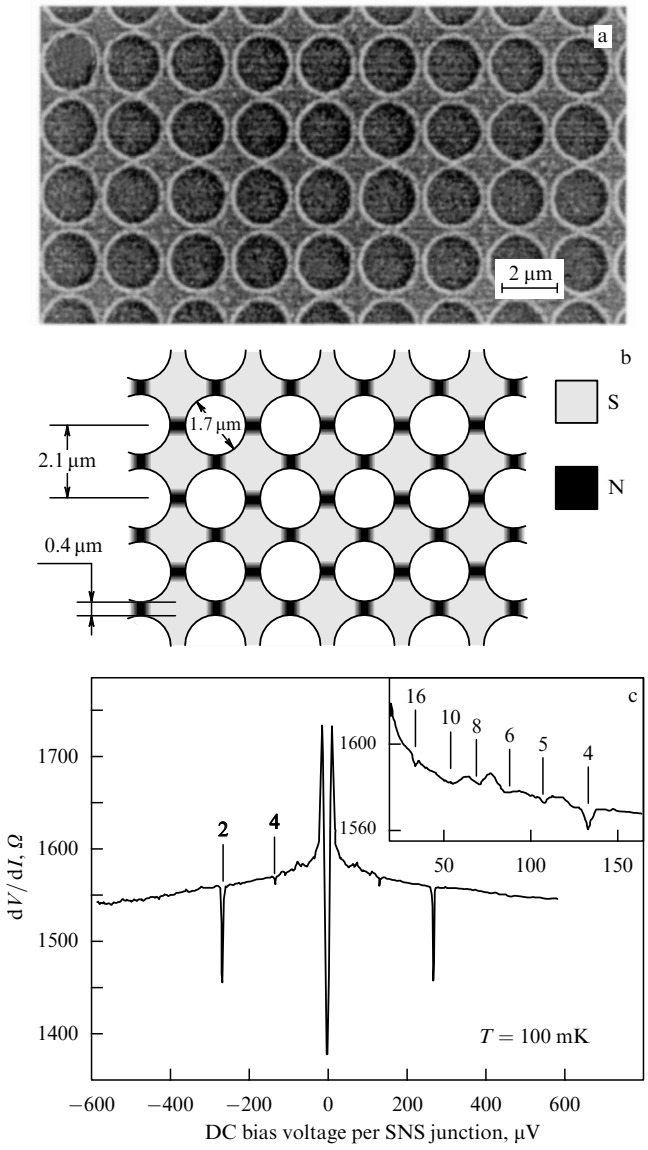

Figure 2. (a) SEM subimage of square lattice of holes made in PtSi film. (b) The layout of a 2D array of SNS junctions showing the dimensions of the structure. Regions of the normal metal constrictions are dark, and the superconducting islands are light gray. (c) Differential resistance of the sample with a 2D array of SNS junctions as a function of dc bias voltage falling at one SNS junction at $T = 100$ mK showing a sharp zero-bias resistance dip followed by above-normal peak. The differential resistance possesses the subharmonic energy gap structure that is seen as symmetrical minima in the range of voltages from ~ 30 μV to ~ 300 μV. The bars indicate the SGS corresponding to integer fractions of 2Δ. The inset reproduces a part of the curve on an expanded voltage scale.

and reaches $R_N \sim 530$ Ω at $V_{ZBA} \sim 140$ μV (R_N is the difference between the resistance of the whole structure with constriction and the resistance of the original film at $T > T_c$). As one can see from the uppermost curves obtained at the highest temperatures, the zero bias anomaly survives even under the condition of fluctuation superconductivity and has the same voltage scale as that at the lowest temperatures. Note that the effective suppression voltage V_{ZBA} is much larger than both the Thouless energy $E_c = \hbar D/L^2 \approx 0.4$ μeV estimated assuming $L = 1$ μm and $k_B T$. In most samples with single SNS junctions, at nonzero biases we observe more or less pronounced symmetric structure in the differential resistance. It is the so-called subharmonic energy gap structure (SGS) originated from the multiple Andreev reflections. In the general case the positions of these features are determined by the condition $eV = \pm 2\Delta/n$, with $n = 1, 2, 3, \ldots$. It should be noted that it follows from the earlier theory [14] describing the subgap current transport in terms of ballistic propagation of quasi-particles that there is no chance to observe the SGS in the case of the high-transparent NS interfaces. The SGS on current-voltage characteristics of single diffusive SNS junctions was observed in Refs [10–13] and has only just been explained in a recent paper [15]. Following the spirit of Nazarov's circuit theory [16], the authors of Ref. [15] show that unlike the ballistic case in long diffusive SNS junctions the SGS survives even for perfect NS interfaces. It occurs owing to coherent impurity scattering

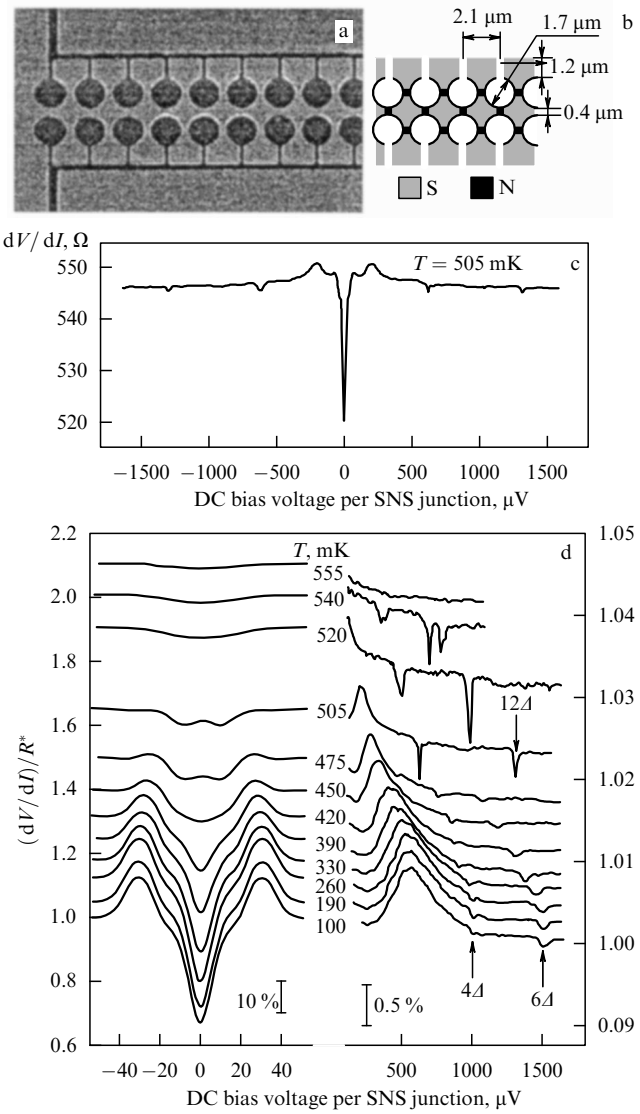

Figure 3. (a) SEM subimage of a series of 20 SNS junctions. (b) The layout of a 1D array of SNS junctions showing the dimensions of the structure. (c) Differential resistance of the sample as a function of the bias voltage falling at one SNS junction at $T = 505$ mK showing a general form of the dependence. The differential resistance reveals symmetrical minima at voltages exceeding 2Δ. (d) Temperature evolution of the normalized differential resistance ($R^* = 546\ \Omega$) vs dc bias voltage divided by 20, that is, the number of SNS junctions in series. (All traces except the lowest trace are shifted up for clarity.) The left panel shows a low-voltage part of the curves. The traces in the right panel are continuations of the ones presented in the left panel to higher voltage. The arrows indicate the above energy gap structure, corresponding to integer multiples of the 2Δ. (Note the change of the scales in the panels.)

of the quasiparticles inside the proximity region that formally corresponds to renormalized value of the interface resistance.

In Figure 2c we present the dependence of the differential resistance on dc bias voltage for one of the 2D arrays of SNS junctions. We have investigated three samples and found the similar behavior. The differential resistance has a minimum at zero bias voltage and shows a maximum at a finite bias voltage of about 10 μV followed by a rapid decrease and eventually a slow decrease at large biases. In comparison with single SNS junctions where the zero-bias resistance dip extends to ~ 140 μV for all 2D arrays of SNS junctions we observe a significant narrowing of ZBA. It is less than 10 μV, with, as for the single SNS junctions, V_{ZBA} being much larger than estimated Thouless energy. At nonzero biases the differential resistance reveals a pronounced and intricate SGS. As seen in Fig. 2c and in the inset to this figure, the dips corresponding to subharmonic numbers $n = 2, 4, 5, 6, 8, 10, 16$ manifest in our case. The precise shape of the structure which we observe for 2D arrays of SNS junctions under study is sample-specific, with even n being commonly more pronounced and some n being absent.

The most striking results are obtained for 1D arrays of SNS junctions. They are a series of SNS junctions, the dimensions of superconducting islands and normal necks being the same as in 2D array. Figure 3c,d shows data taken on one sample representative of others and consisting of 20 SNS junctions in series. At the lowest temperature, as for the SNS systems discussed above, the differential resistance of 1D arrays reveals a minimum at zero bias voltage. The voltage scale of ZBA is close to that for the 2D arrays. But, as temperature increases, we observe a crossover from a zero bias resistance dip to zero bias resistance peak and a dip again at even higher temperatures (see left panel of Fig. 3d). Besides, a number of symmetrical minima is seen, their positions approximately corresponding to 4, 6, and 12 multiples of the superconducting gap. The temperature dependence of the positions of these dips actually reflects the dependence of $\Delta(T)$. It should be stressed that this voltage region corresponds to current density much exceeding the critical current density of initial PtSi film. To our knowledge, it is the first observation of such above energy gap structure (AGS).

The issue to be addressed now is the behavior of the differential resistance at zero bias. For all samples under study at lowest temperatures we observe the dip, with the value of $\Delta R_{SNS}/R_N$ exceeding 10%. It is the so-called excess conductance experimentally observed in all single diffusive SNS junctions [5–13]. ZBA observed in our single SNS junctions is likely to be the result of interplay of nonlocal coherent effects, namely (i) the superposition of multiple coherent scattering at the NS interfaces in the presence of disorder (so-called reflectionless tunneling [17]) and (ii) the electron–electron interaction in the normal part. The latter is one of the important points of recently developed 'circuit theory' when applied to diffusive superconducting hybrid systems [18]. Within this approach based on the use of the nonequilibrium Green function method, the electron–electron interaction induces weak pair potential in the normal metal. It results not only in the change of the resistance, but in a nontrivial distribution of the electrostatic and chemical potentials in the structure as well, that implies nonlocal resistivity in the structure. It is essentially a consequence of coherent nature of Andreev reflection. The most striking feature is, as the results for 2D array of SNS junctions presented in this paper show, that self-averaging is totally absent and coherence of the effects governed by Andreev reflection is maintained over the entire sample. Moreover, in comparison with single SNS junction the manifestation of the effects in multiply connected SNS systems (particularly the SGS in 2D arrays) is far more pronounced. The behavior of ZBA and SGS in 2D arrays of SNS junctions and ZBA and AGS in 1D arrays strongly suggests that the development of a novel theoretical approach is needed which would self-consistently take into account the distribution of currents, potentials and superconducting order parameter. In this connection a recent work [19] should be noted, where the authors have extended the theoretical approach to disordered

systems based on the nonlinear σ-model. An advantage of this approach is, unlike the others where the superconducting order parameter was taken into account just by the boundary conditions for the normal region, that it allows to describe an effect on the superconducting order parameter of disorder in the normal metal and even inside the superconducting region. As a consequence it was shown that the size of superconductor influences the proximity effects. In our case, this may be a probable reason for a drastic decrease of the effective suppression voltage for the ZBA when we turn from a single SNS system to multiply connected SNS junctions.

In summary, we have presented low-temperature transport measurements on single and multiply connected SNS systems fabricated on the basis of superconducting polycrystalline PtSi film. In comparison with single SNS junctions we observe significant narrowing of the ZBA in multiply connected SNS systems: one-dimensional and two-dimensional arrays of SNS junctions. In 2D arrays an appreciable SGS appears, with up to subharmonic number $n = 16$ and with some numbers being lost. One of the most interesting results obtained on 1D arrays consists in the appearance of symmetrical dips on the dependence $\mathrm{d}V/\mathrm{d}I - V$ at dc bias voltages corresponding to some multiples of $2\Delta/e$. Our experiments show that coherent phenomena governed by the Andreev reflection are not only maintained over the macroscopic scale but also manifest novel pronounced effects. It seems that in multiply connected SNS systems the coherent processes on both NS interfaces of the superconducting island of finite size influence each other. To have clear physical understanding of the phenomena observed in mesoscopic multiply connected systems, further theoretical progress is needed.

We would like to acknowledge valuable discussions with M V Feĭgel'man and Yu V Nazarov. This work has been supported by the program "Physics of quantum and wave processes" of the Russian Ministry of Industry, Science and Technology and by the RFBR (Grant 00-02-17965).

References

1. Pannetier B, Courtois H *J. Low Temp. Phys.* **118** 599 (2000)
2. Kastalsky A et al. *Phys. Rev. Lett.* **67** 3026 (1991)
3. Nguyen C, Kroemer H, Hu E L *Phys. Rev. Lett.* **69** 2847 (1992)
4. Van Huffelen W M et al. *Phys. Rev. B* **47** 5170 (1993)
5. Xiong P, Xiao G, Laibowitz R B *Phys. Rev. Lett.* **71** 1907 (1993)
6. Petrashov V T et al. *Phys. Rev. Lett.* **70** 347 (1993)
7. Magnee P H C et al. *Phys. Rev. B* **50** 4594 (1994)
8. Courtois H et al. *Phys. Rev. Lett.* **76** 130 (1996); Charlat P et al. *Phys. Rev. Lett.* **77** 4950 (1996)
9. Jehl X et al. *Phys. Rev. Lett.* **83** 1660 (1999)
10. Kutchinsky J et al. *Phys. Rev. Lett.* **78** 931 (1997)
11. Frydman A, Dynes R C *Phys. Rev. B* **59** 8432 (1999)
12. Hoss T et al. *Phys. Rev. B* **62** 4079 (2000)
13. Kvon Z D et al. *Phys. Rev. B* **61** 11340 (2000)
14. Octavio M et al. *Phys. Rev. B* **27** 6739 (1983); Flensberg K et al. *Phys. Rev. B* **38** 8707 (1988)
15. Bezuglyi E V et al. *Phys. Rev. B* **62** 14439 (2000)
16. Nazarov Yu V *Phys. Rev. Lett.* **73** 1420 (1994); *Superlattices Microstr.* **25** 1221 (1999)
17. Van Wees B J et al. *Phys. Rev. Lett.* **69** 510 (1992); Beenakker C W J *Phys. Rev. B* **46** 12841 (1992); Marmorkos I K, Beenakker C W J, Jalabert R A *Phys. Rev. B* **48** 2811 (1993)
18. Nazarov Y V, Stoof T H *Phys. Rev. Lett.* **76** 823 (1996); Stoof T H, Nazarov Yu V *Phys. Rev. B* **53** 14496 (1996)
19. Yurkevich I V, Lerner I V *Phys. Rev. B* **63** 064522 (2001)

Nonlocal fluctuation effects in clean superconductor

A A Varlamov, D V Livanov, G Savona

Abstract. The theory of fluctuation conductivity for an arbitrary impurity concentration including ultra-clean limit ($T\tau \gg \sqrt{T_c/T - T_c}$) is developed. It is demonstrated that the formal divergency of the fluctuation density of states contribution obtained previously for the clean case is removed by the correct treatment of the nonlocal ballistic electron scattering. We show that in the ultra-clean limit the density-of-states quantum corrections are canceled by the Maki – Thompson term and only classical paraconductivity remains.

As is well known, the first-order fluctuation corrections to conductivity in the vicinity of superconducting transition are presented by the Aslamazov – Larkin (AL), Maki – Thompson (MT) and density of states (DOS) contributions. The first one has the simple physical meaning of the direct charge transfer by the fluctuation pairs themselves and can be easily derived from the phenomenological time-dependent Ginzburg – Landau equation [1]. In this sense, it is a result characteristic of the classical electron theory, while Maki – Thompson and DOS contributions have the purely quantum origin and can be calculated in the framework of the microscopic approach only [2].

The character of the electron scattering plays a very special role for the manifestation of fluctuation effects. In the BCS theory of superconducting alloys the only criterion of the metal purity exists: it is the ratio between the Cooper pair 'size' (zero temperature coherence length of pure metal, ξ_0) and the electron mean free path ℓ. If the alloy is dilute ($\ell \gg \xi_0$), the Cooper pairs motion is ballistic and impurities do not manifest themselves in superconductor properties. In the opposite case, $\ell \ll \xi_0$, the Cooper pair motion has the diffusive character and the role of the effective Cooper pair size is played by the renormalized coherence length $\xi' = \sqrt{\ell\xi_0}$. The relative magnitude of fluctuation effects, which is determined by the Ginzburg – Levanyuk number, is proportional to $(a/\xi)^n$ (a is an interatomic distance and $n > 0$ depends on the effective dimensionality of the electron spectrum) and it grows for impure systems.

Dealing with the superconductor electrodynamics in fluctuation regime it is necessary to remember that in the vicinity of the critical temperature, the Ginzburg – Landau coherence length $\xi_{GL}(T) = \xi_0/\sqrt{\varepsilon}$ plays the role of fluctuation Cooper pair effective size (where the reduced temperature $\varepsilon = (T - T_c)/T_c$). So the case of dilute metal ($\ell \gg \xi_0$) in the vicinity of the transition could be formally subdivided on clean, which is still local ($\xi_0 \ll \ell \ll \xi_{GL}(T)$) and ultra-clean, non-local ($\xi_{GL}(T) \ll \ell$) limits. In terms of the used in the theory of disordered alloys parameter $T\tau$ the same three domains can be written down as $T\tau \ll 1$; $1 \ll T\tau \ll 1/\sqrt{\varepsilon}$ and $1/\sqrt{\varepsilon} \ll T\tau$. (We use units $k_B = \hbar = c = 1$). The latter case

A A Varlamov, G Savona Istituto Nazionale di Fisica della Materia-Unità "Tor Vergata", Dipartimento di Scienze e Tecnologie Fisiche ed Energetiche, Università di Roma "Tor Vergata", via di Tor Vergata 110, 00133 Roma, Italy
D V Livanov Moscow State Institute of Steel and Alloys, Leninskiĭ prosp. 4, 117936 Moscow, Russian Federation